

Synthesis and Properties of Azulene-substituted Donor–Acceptor Chromophores Connected by Arylamine Cores

Taku Shoji,^{*,[a]} Erika Shimomura,^[a] Mitsuhisa Maruyama,^[a] Akifumi Maruyama,^[a] Shunji Ito,^[b] Tetsuo Okujima,^[c] Kozo Toyota,^[d] and Noboru Morita^[d]

Keywords: Azulene / Arylamine / π -Conjugate system / Cycloaddition / Redox chemistry /

1-Ethynylazulenes connected by several arylamine cores reacted with tetracyanoethylene (TCNE) and 7,7,8,8-tetracyanoquinodimethane (TCNQ) in a formal [2 + 2] cycloaddition–cycloreversion reaction to afford the corresponding tetracyanobutadiene (TCBD) and dicyanoquinodimethane (DCNQ) chromophores, respectively, in excellent yields. The intramolecular charge-transfer (ICT) characters between the donor (azulene and arylamine cores) and acceptor (TCBD and DCNQ units) moieties were investigated by UV/Vis spectroscopy and theoretical calculations.

The redox behavior of the novel TCBD and DCNQ derivatives was examined by cyclic voltammetry (CV) and differential pulse voltammetry (DPV), which revealed their multistep electrochemical reduction properties. Moreover, a significant color changes were observed by visible spectroscopy under the electrochemical reduction conditions.

[a] Department of Chemistry, Faculty School of Science, Shinshu University, Matsumoto 390-8621, Japan
Fax: +81-263-37-2476
E-mail: tshoji@shinshu-u.ac.jp

[b] Graduate School of Science and Technology, Hirosaki University, Hirosaki 036-8561, Japan

[c] Department of Chemistry and Biology, Graduate School of Science and Engineering, Ehime University, Matsuyama 790-8577, Japan

[d] Department of Chemistry, Graduate School of Science, Tohoku University, Sendai 980-8578, Japan
Supporting information for this article is available on the WWW under <http://www.eurjoc.org/> or from the author.

Introduction

Arylamine derivatives are very important compounds for the development of organic electronic materials, such as light emitting diodes (LED),^[1] semiconductors,^[2] solar cells,^[3] memory devices,^[4] and so on. Donor–acceptor derivatives possessing the arylamine moieties have also attracted much interest due to their potentials as organic electronics.^[5] Therefore, a variety of these derivatives have been synthesized as shown in the literatures.

Recently, Diederich *et al.* reported that a variety of alkynes substituted by arylamine moieties reacted with tetracyanoethylene (TCNE) and 7,7,8,8-tetracyanoquinodimethane (TCNQ) to give tetracyanobutadiene (TCBD) and dicyanoquinodimethane (DCNQ) derivatives, respectively, in excellent yields.^[6] They have also reported that the new chromophores obtained by the reaction have potentials for the application to third-order nonlinear optics, liquid crystals, and molecular batteries. In the meanwhile, Michinobu *et al.* have reported the synthesis of polymers with multiple TCBD and DCNQ moieties embedded by arylamine units.^[7] The polymers with multiple donor–acceptor moieties might become promising candidates for the application to the semiconductors in organic photovoltaic devices, nonlinear optical materials, and ion sensors.

We have also reported the synthesis and electrochemical properties of TCBD and DCNQ derivatives with azulenyl,^[8] 2-oxo-2*H*-cyclohepta[*b*]-3-furyl,^[9] and ferrocenyl^[10] substituents, which have been prepared by the [2 + 2] cycloaddition–cycloreversion reaction of the corresponding acetylene derivatives with TCNE and TCNQ, respectively. Particularly, azulene-substituted TCBDs represent significant color changes with high reversibility among them under the redox conditions. As well as the azulenyl, 2-oxo-2*H*-cyclohepta[*b*]-3-furyl, and ferrocenyl substituents, that were examined by our groups as the end groups, arylamino groups also possess strong electron-donating properties with high reactivities. Thus, the acetylene derivatives connected by the arylamine cores are expected to afford a new series of chromophores with multiple donor–acceptor units by the sequential [2 + 2] cycloaddition–cycloreversion sequence with TCNE and TCNQ. Furthermore, novel chromophores with multiple donor–acceptor units may exhibit multistage redox behavior by the redox reaction of both donor (i.e., azulene and arylamines) and acceptor moieties.

We describe herein the synthesis of novel azulene-substituted acetylene derivatives connected by several arylamine cores including multiple 1-ethynylazulene units utilizing Sonogashira–Hagihara cross-coupling reaction, as well as the preparation of the novel TCBD and DCNQ chromophores by the [2 + 2] cycloaddition–cycloreversion reaction of the azulene-substituted acetylene derivatives with TCNE and TCNQ, respectively. The electronic properties of the novel TCBD and DCNQ derivatives connected by the arylamine cores were investigated by absorption spectroscopy, electrochemical analysis and theoretical calculations.

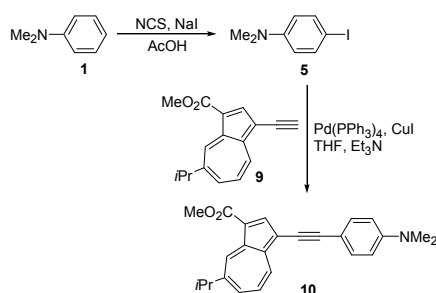
Results and Discussion

Synthesis

Iodine substituent is a very important functional group in the transition-metal-catalyzed cross-coupling reaction of aromatic compounds, because aryl iodides possess higher reactivity compared with the corresponding bromides and chlorides.^[11] However, difficulty in the preparation process declines the general usability of the aryl iodides. Preparation of aromatic iodides is often carried out effectively by using the iodination reagents, such as I₂,^[12] ICl,^[13] and *N*-iodosuccinimide (NIS)^[14]. However, most of the reagents are toxic or expensive, and/or the reaction with the reagents often requires severe reaction conditions as found in the literatures.^{12,13,14} We have recently developed an efficient iodination procedure using NaI in the presence of *N*-chlorosuccinimide (NCS).^[8e, 9a, 15] Thus, we have examined the preparation of the starting iodoarylamines **5–8** taking the strategy for the iodination of the arylamines **1–4**, that require for the next palladium-catalyzed cross-coupling reaction.

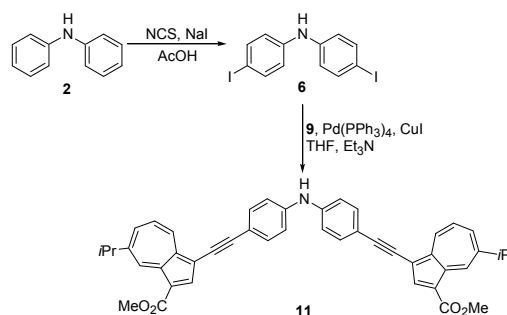
Thus, the reaction of **1** with NaI/NCS in acetic acid and subsequent chromatographic purification of the reaction mixture on silica gel afforded the desired **5**^[15] in 80% yield (Scheme 1). Likewise, the reaction of **2** and **3** with NaI/NCS afforded the presumed iodination products **6**^[16] and **7**^[17] in 97% and 71% yield, respectively (Schemes 2 and 3). Triiodide derivative **8**^[18] was also obtained by the similar reaction of **4** with NaI/NCS in 95% yield (Scheme 4). The yields of the products in these reactions were comparable to those of the reactions with NIS reported in the literatures. Thus, the present procedure has great advantages for the preparation of iodoarylamines, with respect to the product yields and cost-effectiveness.

Preparation of 1-ethynylazulenes connected by arylamine cores **10–14** was accomplished by palladium-catalyzed alkylation of 1-ethynylazulene **9**^[8, 19] with the corresponding iodoarylamines **5–8** under Sonogashira–Hagihara conditions.^[20] The cross-coupling reaction of **5** with **9** in the presence of Pd(PPh₃)₄ as a catalyst in THF/Et₃N at 50 °C gave methyl 3-(4-dimethylaminophenylethynyl)-7-isopropylazulene-1-carboxylate (**10**) in 99% yield.

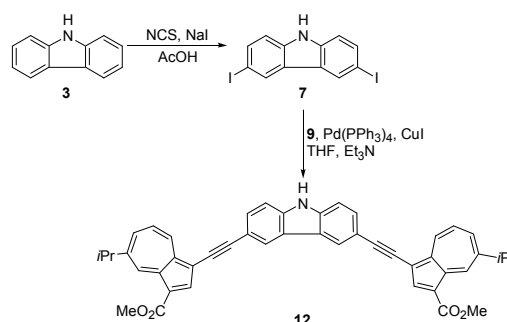


Scheme 1. Synthesis of compound **10**.

The cross-coupling reaction of **6** with **9** using Pd(PPh₃)₄ as a catalyst and subsequent chromatographic purification on silica gel afforded the desired 4,4'-bis(1-methoxycarbonyl-7-isopropyl-3-azulenylethynyl)diphenylamine (**11**) in 94% yield (Scheme 2). The reaction of **7** with **9** afforded **12** in 85% yield (Scheme 3).

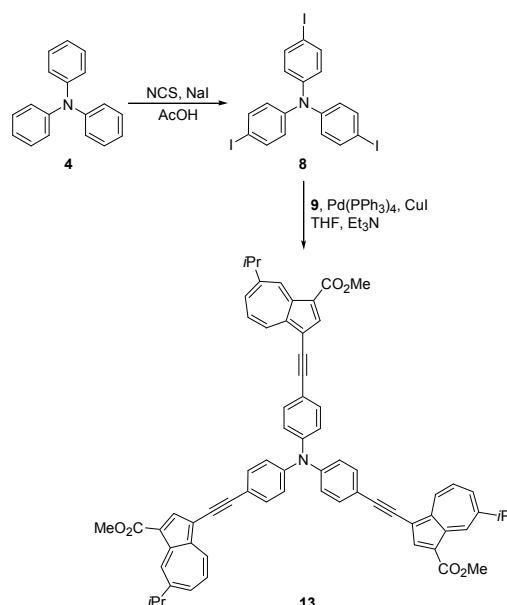


Scheme 2. Synthesis of compound **11**.



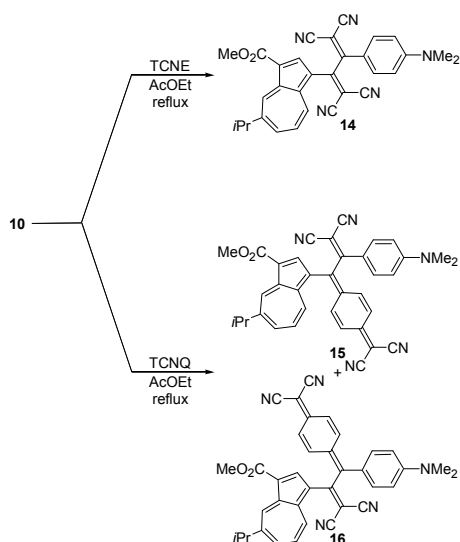
Scheme 3. Synthesis of compound **12**.

The cross-coupling reaction of **8** with **9** in the presence of the Pd-catalyst afforded **13** in 90% yield (Scheme 4). These acetylene derivatives **10–13** possess fair solubility toward common organic solvents (e.g., chloroform, dichloromethane, and so on). Moreover, they are stable and showing no decomposition, even after several weeks at room temperature. Thus, these acetylene derivatives are utilized in further transformations for the synthesis of the novel TCBD and DCNQ derivatives owing to their considerable stability and solubility.



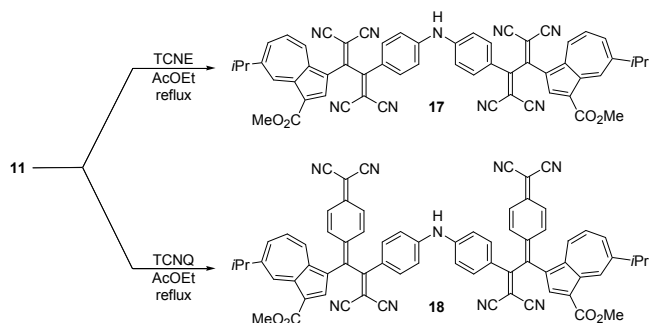
Scheme 4. Synthesis of compound **13**.

The [2 + 2] cycloaddition–cycloreversion sequence of **10–13** with TCNE and TCNQ was applied for the synthesis of the novel TCBD and DCNQ derivatives. The reaction of **10** with TCNE in refluxing ethyl acetate yielded **14** in 97% yield as a sole product. On the other hand, compounds **15** and **16** were generated in 43% and 48% yields, respectively, by the reaction of **10** with TCNQ (Scheme 5). Recently, Diederich et al. have reported the regioselectivity in the [2 + 2] cycloaddition of C≡C triple bond with TCNQ correlated to the electron-donating property of the substituent on the ethynyl group.^[21] Thus, the less selectivity for the generation of **15** and **16** suggests 1-azulenyl group in **10** possesses almost same electron-donating nature with that of *N,N*-dimethylanilino (DMA) group.

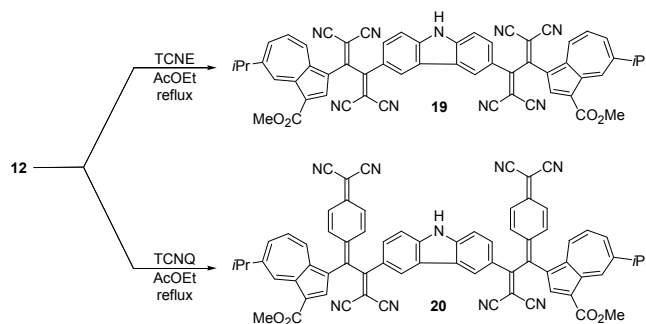


Scheme 5. Reaction of **10** with TCNE and TCNQ.

The double-addition of TCNE to **11** gave **17** in 98% yield by stirring in the refluxing ethyl acetate. The DCNQ chromophore **18** was also prepared by the one-pot formal [2 + 2] cycloaddition–cycloreversion reaction of **11** with TCNQ in 91% yield (Scheme 6). The TCBD and DCNQ chromophores with carbazole unit **19** and **20** were obtained in 92% and 84% yields, respectively, by the [2 + 2] cycloaddition–cycloreversion reaction of acetylene precursor **12** with TCNE and TCNQ, respectively (Scheme 7).

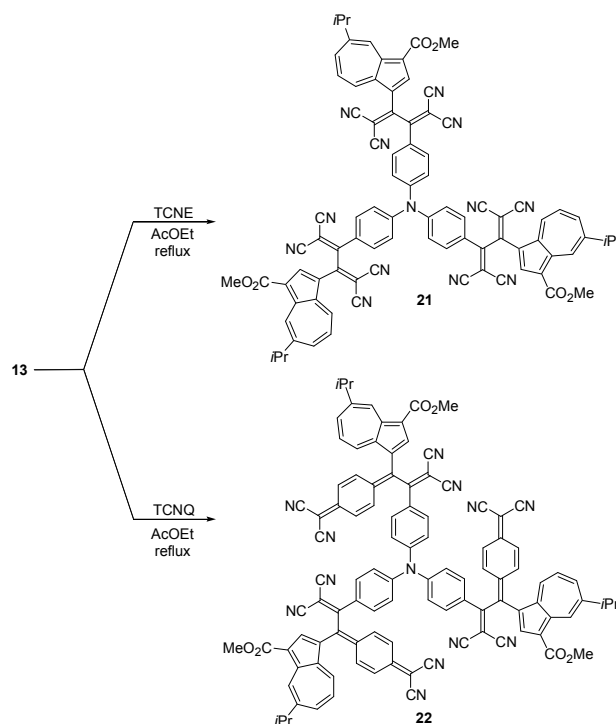


Scheme 6. Reaction of **11** with TCNE and TCNQ.



Scheme 7. Reaction of **12** with TCNE and TCNQ.

Tris-adducts **21** and **22** were obtained in excellent yields (**21**: 90%; **22**: 87%) by the cycloaddition reaction of TCNE and TCNQ, respectively, with the corresponding alkyne **13** followed by the cycloreversion reaction (Scheme 8). These novel TCBD and DCNQ derivatives **14–22** are obtained as stable crystals and can be storable in crystalline state under ambient conditions.



Scheme 8. Reaction of **13** with TCNE and TCNQ.

Properties

These new compounds were fully characterized by the spectral data, as shown in the Supporting Information. Assignment of peaks in the ¹H and ¹³C NMR spectra of the compounds was accomplished by NOE, and COSY, HMQC and HMBC experiments. Mass spectra of **10–22** ionized by FAB showed the correct molecular ion peaks. The characteristic stretching vibration band of the acetylene moiety of **10–13** was observed at $\nu_{\max} = 2196\text{--}2197\text{ cm}^{-1}$ in their IR spectra. The TCBD and DCNQ derivatives **14–22** exhibited a characteristic C≡N stretching band at $\nu_{\max} = 2202\text{--}2224\text{ cm}^{-1}$ in their IR spectra. These results are consistent with the structures of the products.

UV/Vis spectra of **10–22** are shown in Figures 1, 2, and 3. Their absorption maxima and coefficients ($\log \epsilon$) of TCBDs and DCNQs **14–22** in dichloromethane and in hexane including certain amount of dichloromethane to maintain the solubility of the product are summarized in Table 1. The UV/Vis spectra of the acetylene derivatives **10–13** showed characteristic weak absorption bands arising from the azulene system in the visible region. Although the extinction coefficients increased with the number of substituted azulene rings, absorption bands in the visible region of these compounds resemble each other (Figure 1). These results suggest that connection of multiple 1-ethynylazulene moieties in the arylamine cores does not exhibit effective π -conjugation in these cases.

Table 1. Absorption maxima [nm] and their coefficients ($\log \epsilon$) of TCBDs and DCNQs **14–22** in dichloromethane and in hexane,^[a–c] and TCBD **23**, DCNQ **24**, and **25** as references.

Sample	λ_{\max} ($\log \epsilon$) in CH ₂ Cl ₂	λ_{\max} ($\log \epsilon$) in hexane
14	474 (4.49)	459 (4.49) ^[a]
15	631 (4.37)	593 (4.36) ^[b]
16	689 (4.52)	619 (4.48) ^[b]
17	489 (4.81)	459 (4.49) ^[a]
18	628 (4.71)	617 (4.71) ^[c]
19	456 (4.58)	449 (4.55) ^[a]
20	637 (4.70)	626 (4.69) ^[c]
21	503 (4.86)	488 (4.84) ^[a]
22	628 (4.85)	617 (4.83) ^[c]
23 ^[8a]	462 (4.04)	–
24 ^[8b]	641 (4.43)	598 (4.42) ^[b]
25 ^[22]	676 (4.56)	600 ^[b]

Dichloromethane was included in hexane to maintain solubility of the compounds. [a] Measured in 20% CH₂Cl₂/hexane. [b] Measured in 10% CH₂Cl₂/hexane. [c] Measured in 50% CH₂Cl₂/hexane.

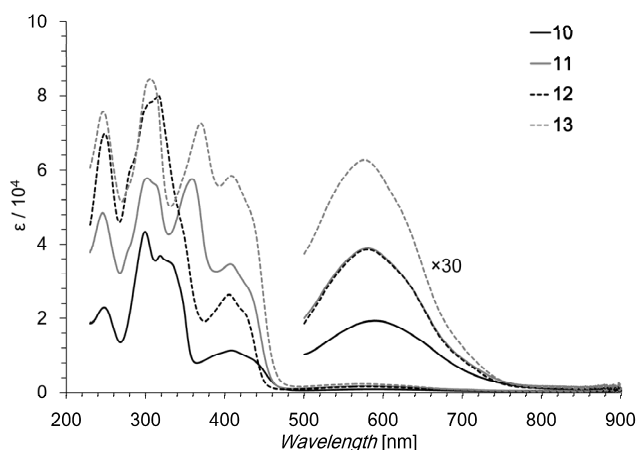
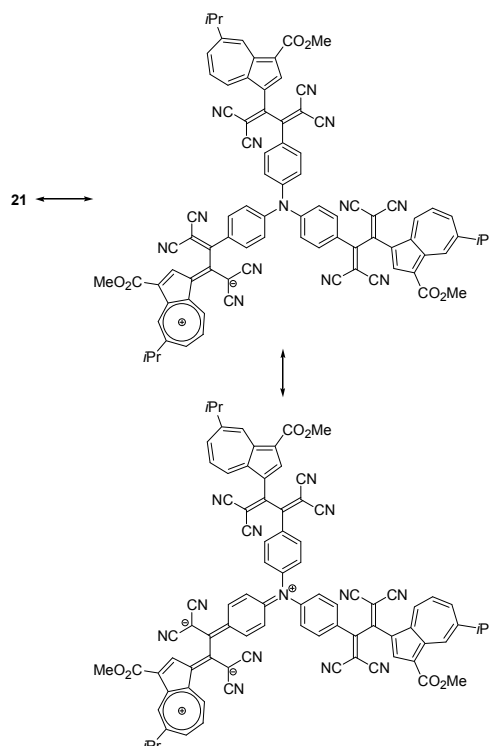


Figure 1. UV–visible spectra of **10** (black line), **11** (gray line), **12** (broken black line), **13** (broken gray line) in dichloromethane.

TCBD **14** exhibited a broad absorption band at $\lambda_{\max} = 474$ nm. Likewise, TCBD **17** with a diphenylamine core also displayed a broad and strong CT absorption band at $\lambda_{\max} = 489$ nm. TCBD **21** with a triphenylamine core showed a strong absorption band at $\lambda_{\max} = 503$ nm. The bathochromic shift in the absorption maxima of TCBDs **14**, **17**, and **21** in accordance with the increment of the number of substituted TCBD moieties suggest the π -conjugation of the TCBD moieties with the amine cores as illustrated in Scheme 9. However, absorption maxima of TCBD **19** ($\lambda_{\max} = 456$ nm) exhibited a hypsochromic shift compared to those of **14**, **17**, and **21**. The absorption maxima of **19** were nearly equal to that of the simpler TCBD derivative **23** ($\lambda_{\max} = 462$ nm), although the

extinction coefficients still show the trend of increase by the number of TCBD units. These effects are suggested by the less effective π -conjugation between the central nitrogen atom and the TCBD units in **19**, due to the less electron-donating properties of the carbazole spacer to form a quinoidal structure by the resonance forms.



Scheme 9. Presumed resonance structure of **21**.

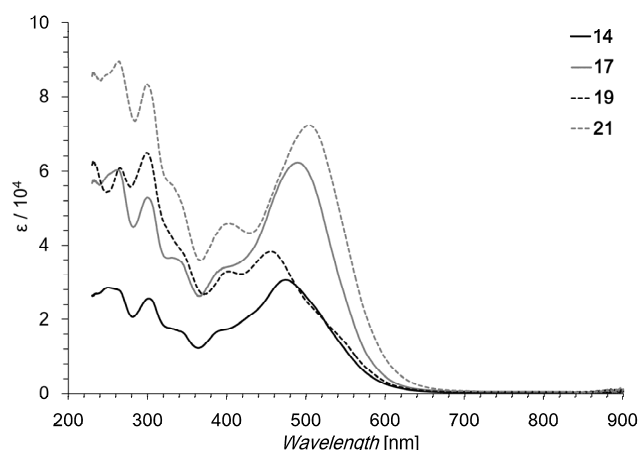


Figure 2. UV–visible spectra of TCBDs **14** (black line), **17** (gray line), **19** (broken black line), and **21** (broken gray line) in dichloromethane.

The DCNQ chromophores **15** and **16** exhibited a strong absorption band at $\lambda_{\max} = 631$ nm and $\lambda_{\max} = 689$ nm in dichloromethane, respectively. Whereas the longest wavelength absorption maximum of **15** in the same spectral region resembles with that of **24** at $\lambda_{\max} = 641$ nm, absorption maximum of **16** ($\lambda_{\max} = 689$ nm) in dichloromethane showed similar value with that of simpler DCNQ **25** ($\lambda_{\max} = 676$ nm).^[22] These results might be attributed to the effectiveness of the ICT between the DCNQ unit and directly conjugated DMA groups, rather than the cross

conjugated dicyanomethylidene unit. The absorption maxima of **18**, **20**, and **22** (**18**: 628 nm; **20**: 637 nm; **22**: 628 nm) were nearly equal to that of **15**, although the extinction coefficients were in proportion to the number of DCNQ units.

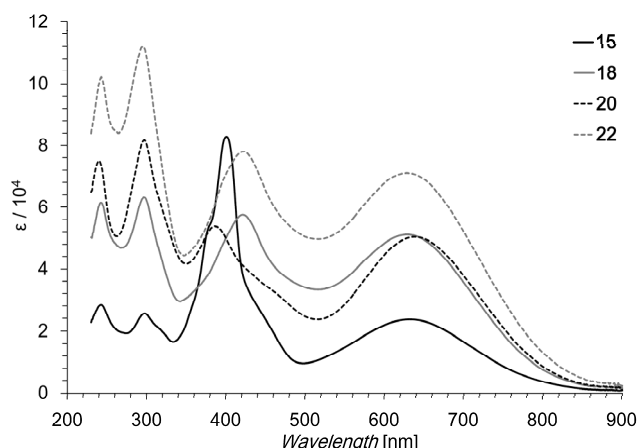


Figure 3. UV-visible spectra of DCNQ **15** (black line), **18** (gray line), **20** (broken black line) and **22** (broken gray line) in dichloromethane.

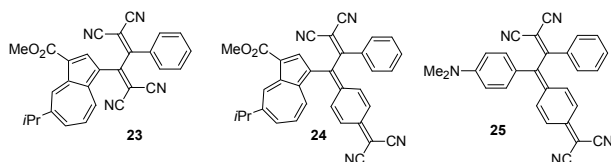


Figure 4. TCBD and DCNQ derivatives **23**–**25**.

Most of the TCBD and DCNQ derivatives showed solvatochromism, when the solvent was changed from dichloromethane to hexane including certain amount of dichloromethane. A noticeable spectral feature of **16** is the presence of a distinct absorption band at 689 nm in dichloromethane, in which compound **16** exhibits blue-shifts by 70 nm ($\lambda_{\text{max}} = 619$ nm) in less polar 10% dichloromethane/hexane, suggesting the ICT nature of this band (Figure 5).^[23] The shift value of DCNQs is larger than that of the corresponding TCNE-adducts (TCBDs). These indicate that DCNQs possess high-polarity compared to the corresponding TCBDs, respect to the results from the measurement of UV/Vis spectra.

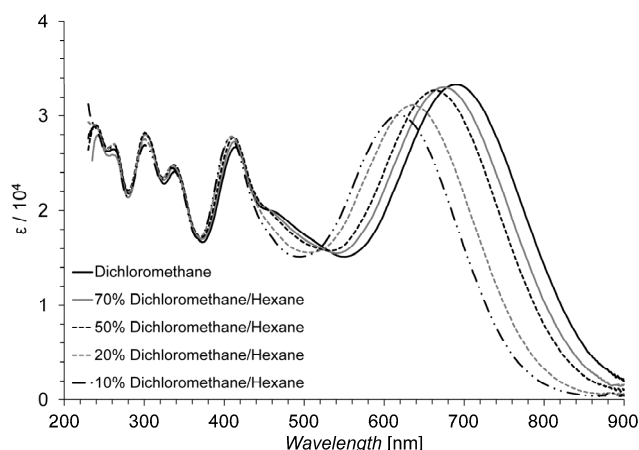


Figure 5. UV-visible spectra of DCNQ **16** in dichloromethane and dichloromethane/hexane.

To elucidate the nature of the absorption bands of **14**, **15**, and **16**, time-dependent density functional theory (TD-DFT) calculations at the B3LYP/6-31G(d) level were carried out on model compounds **14'**, **15'**, and **16'**, in which the isopropyl group of **14**, **15**, and **16** was replaced with H-group.^[24] The frontier Kohn–Sham orbitals of these compounds are shown in the Supporting Information. Judging from a comparison between the experimental and the theoretical UV/Vis spectra, the absorption maxima of **14** in the visible region could be assigned to the transition originated from the HOMO located on DMA and the HOMO–1 located at azulene ring to the LUMO that was located on the TCBD moiety. Thus, the broad absorption at $\lambda_{\text{max}} = 474$ nm of **14** could be concluded to the overlapping of the CT absorptions from the 1-azulenyl and DMA moieties to the TCBD unit.

Molecular orbital calculations performed on **15'** by using the B3LYP/6-31G(d) density functional theory exhibited that the absorption band at $\lambda_{\text{max}} = 595$ nm of **15** is considered as overlap of some transitions, which originated from the HOMO located on the 1-azulenyl group and HOMO–1 located on the DMA group to the LUMO and LUMO+2 located on the DCNQ moiety. The π – π^* transitions of the substituted azulene moiety was confirmed from the calculations of **15'** observed as the computed value at $\lambda_{\text{max}} = 568$ nm with relatively weak strength. ICT of **16'** was also confirmed by the B3LYP/6-31G(d) density functional calculations that the longest absorption band was arisen from the overlapping of some transitions as shown in Table 2. Difference from the results on **15'** was the effective contribution of HOMO→LUMO (i.e., transition between attached DMA and DCNQ moieties), compared with that from 1-azulenyl group to DCNQ. These results suggest that the longest wavelength absorption band has characteristics depending on the substituted aryl group conjugated directly with DCNQ moiety.

Table 2. Electronic transitions for **14'**, **15'**, and **16'** derived from the computed values based on B3LYP/6-31G(d) method and experimental values from **14**, **15**, and **16**.

Sample	Experimental	Computed Value	
	λ_{max} (log ϵ)	λ_{max} (strength)	Composition of band ^[a]
14'	474 (4.49) ^[b]	493 (0.0738)	H→L (0.90)
		480 (0.0168)	H–1→L (0.32)
			H–1→L+1 (0.83)
		457 (0.0712)	H→L+1 (0.37)
15'	593 (4.36) ^[c]	595 (0.0358)	H–1→L (0.84)
		568 (0.0070)	H–1→L+2 (0.39)
		515 (0.4537)	H→L (0.97)
			H→L+1 (0.97)
			H→L (0.73)
16'	619 (4.48) ^[c]	605 (0.3451)	H–1→L+2 (0.52)
			H→L (0.78)
			H→L+2 (0.50)
		566 (0.0099)	H→L+1 (0.98)
		544 (0.1058)	H–2→L (0.23)
			H–1→L (0.91)

[a] H = HOMO; L = LUMO. [b] Measured in CH₂Cl₂. [c] Measured in 10% CH₂Cl₂/hexane.

Electrochemistry

To clarify the electrochemical properties, the redox behavior of **14**–**22** was examined by CV and DPV. Measurements were carried out with a standard three-electrode configuration. Tetraethylammonium perchlorate (0.1 M) in benzonitrile was used as a supporting electrolyte with platinum wire and disk as auxiliary and working electrodes, respectively. All measurements were carried out under an argon atmosphere, and potentials were related to an Ag/AgNO₃ reference electrode and Fc/Fc⁺ as an internal

reference, which discharges at +0.15 V under these conditions for the measurements. A cyclic voltammogram for the reduction of **14** is shown in Figure 6. The redox potentials (in volts vs. Ag/AgNO₃) of **14–22** are summarized in Table 1.

Table 3. Redox potentials of TCBDs and DCNQs **14–22** bearing arylamine cores,^[a,b] and TCBD **23** and DCNQ **24** as references.

Sample	Method	E_1^{red} [V]	E_2^{red} [V]	E_3^{red} [V]	E_4^{red} [V]
14	CV	-0.78	-1.09		
	(DPV)	(-0.76)	(-1.07)	(-1.98)	
15	CV	-0.54	-0.67		
	(DPV)	(-0.52)	(-0.65)	(-1.94)	
16	CV	-0.53	-0.67		
	(DPV)	(-0.51)	(-0.65)	(-1.87)	
17	CV	-0.63	-0.72	-1.06	
	(DPV)	(-0.61)	(-0.70)	(-1.04)	(-1.96)
18	CV	-0.51	-0.64		
	(DPV)	(-0.49)	(-0.62)	(-1.98)	
19	CV	-0.64	-0.70	-1.05	
	(DPV)	(-0.62)	(-0.68)	(-1.03)	(-1.96)
20	CV	-0.50	-0.64		
	(DPV)	(-0.48)	(-0.62)	(-2.00)	
21	CV	-0.58	-0.68	-1.02	
	(DPV)	(-0.56)	(-0.66)	(-1.00)	(-1.94)
22	CV	-0.46	-0.61		
	(DPV)	(-0.44)	(-0.59)	(-1.94)	
23	CV	-0.61	-1.03		
	(DPV)	(-0.59)	(-1.01)	(-1.95)	
24	CV	-0.43	-0.59		
	(DPV)	(-0.41)	(-0.57)	(-0.90)	(-1.93)

[a] V vs. Ag/AgNO₃, 1 mM in benzonitrile containing Et₄NClO₄ (0.1 M), Pt electrode (internal diameter: 1.6 mm), scan rate = 100 mVs⁻¹, and internal reference (Fc/Fc⁺ = +0.15 V). [b] Half-wave potential $E^{\text{red}} = (E_{\text{pc}} + E_{\text{pa}})/2$ on CV, E_{pc} and E_{pa} correspond to the cathodic and anodic peak potentials, respectively.

The oxidation of these compounds exhibited voltammograms that were characterized by irreversible oxidation waves on CV, although reversible oxidation wave was frequently observed in the arylamine derivatives due to the generation of stabilized radical cationic species by the electron removal from the nitrogen atom. It might be attributable to the destabilization of radical cationic species by the electron-withdrawing TCBD and DCNQ units.

Electrochemical reduction of TCBD derivatives **14**, **17**, **19**, and **21** displayed a reversible two- or three-stage wave, which contains multi-electron transfer in some cases. As shown in Table 3, the first reduction potentials of **14**, **17**, **19**, and **21** depend on the number of TCBD units in the molecule. Electrochemical reduction of **14** showed a reversible two-step reduction wave with the half-wave potentials of -0.78 V and -1.09 V upon CV, which can probably be attributed to the formation of a stabilized radical anionic and a dianionic species, respectively (Figure 6).

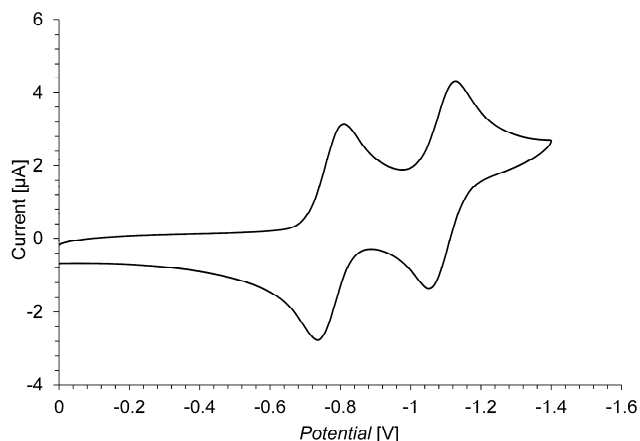


Figure 6. Cyclic voltammogram of **14** (1 mM) in benzonitrile containing Et₄NClO₄ (0.1 M) as a supporting electrolyte; scan rate = 100 mVs⁻¹.

A reversible three-stage wave was observed by CV in bis-adducts **17** (-0.63 V, -0.72 V, and -1.06 V) and **19** (-0.64 V, -0.70 V, and -1.05 V), in which the third reduction waves were a two-electron transfer in one step to form a tetraanionic species. The electrochemical reduction of **21** also exhibited a reversible three-step reduction wave, whose potentials were identified at -0.58 V, -0.68 V, and -1.02 V by CV. The first reduction potentials of **14**, **17**, **19**, and **21** decreased in the order of the number of TCBD units. This indicates that the connection of multiple TCBD units lowers the LUMO-level and increases the π -accepting property by the effective π -conjugation with the arylamine cores.

Electrochemical reduction of DCNQs **15**, **16**, **18**, **20**, and **22** also showed a reversible two-stage reduction wave on CV, which could be attributed to the formation of a radical anionic, dianionic species, and so on. The DCNQs **15**, **16**, **18**, **20**, and **22** exhibited more negative reduction potentials compared with those of the corresponding TCBD chromophores. These results are ascribed to the higher electron-accepting nature of the DCNQ moieties than that of the corresponding TCBD derivatives. The DMA-substituted TCBD **14** and DCNQ **15** showed more negative reduction potentials than those of the corresponding **23** ($E_1^{\text{red}} = -0.61$ V) and **24** ($E_1^{\text{red}} = -0.43$ V). These results should be assumed that the DMA moiety increases LUMO-level due to its higher electron-donating property than that of the phenyl substituent.

We have reported the synthesis of various azulene-substituted redox-active chromophores with the aim of creating stabilized electrochromic materials.^[25] In these studies, the TCBD units connected with π -electron systems exhibit stabilized electrochromism with strong absorptions in visible and near-infrared regions in their two-electron-reduced state. Thus, to examine the color changes during the electrochemical reactions, spectral changes of the new TCBD and DCNQ derivatives were monitored by visible spectroscopy. Constant-current reduction was applied to the solutions of chromophores **14–22**, with a platinum mesh as a working electrode and a wire counter-electrode, and visible spectra were measured in benzonitrile containing Et₄NClO₄ (0.1 M) as a supporting electrolyte at room temperature under the electrochemical reduction conditions (see the Supporting Information).

The longest absorption band of TCBD **14** at around 470 nm gradually decreased along with a development of the new absorption band at around 680 nm. The color of the solution gradually changed from red to yellow during the electrochemical reduction, but reverse oxidation of the yellow-colored solution did not regenerate the spectrum of **14**, although good reversibility was observed in the two-step reduction on CV. The poor reversibility of the color changes might be attributable to the instability of the presumed dianionic species, due to the destabilization by the electron-donating DMA unit. The longest absorption bands of the TCBD derivatives with arylamine cores **17**, **19**, and **21** also gradually decreased, and the color of the solution changed from red to yellow during the electrochemical reduction. The reversible oxidation of the yellow solutions also did not regenerate the spectrum of the corresponding starting compounds (Figure 7).

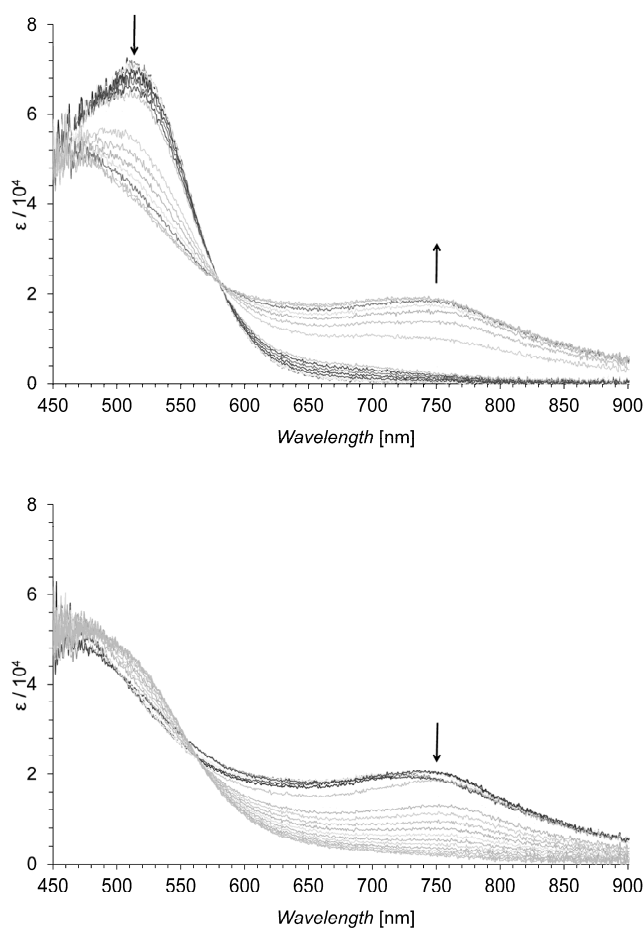


Figure 7. Continuous change in the UV–visible spectrum of **17**: constant-current electrochemical reduction (100 μA , top) and reverse oxidation of the reduced species (100 μA , bottom) in benzonitrile containing Et_4NClO_4 (0.1 M) at 30 sec intervals.

When the spectral changes of DCNQ **15** were monitored during the electrochemical reduction, the absorption in the visible region gradually decreased with the development of new absorption bands at 755 nm and 860 nm, which are spreading over the near-infrared region (Figure 8, top). The color change should be attributable to the formation of anionic species formed by the two-electron reduction of **15** (Figure 8, bottom). Reverse oxidation of the reduced species decreased the new absorption bands and regenerated the original color of **15**. Presumed redox behavior of **15** is illustrated in Scheme 10. As suggested by the results on the CV, the color change of **15** should be ascribed by the two electron reduction of the DCNQ unit to form dianionic species, which could be described as closed-shell form as illustrated in Scheme 10. The longest absorption band of DCNQ **16** gradually decreased, and the color of the solution changed from dark-green to yellow during the electrochemical reduction. Reversible oxidation of the yellow-colored solution regenerated the spectra of the corresponding original compound, but incompletely. The absorption bands of **17** in the visible region disappeared along with increasing the new absorption maxima around 750 nm during the electrochemical reduction. The color of the solution gradually changed from red to yellow during the electrochemical reduction. The reverse oxidation of the intermediary yellow solution did not regenerate the parent spectrum of **17**. When the visible spectra of **18** were measured under electrochemical reduction conditions, absorption of **18** in the visible region gradually decreased along with a color change from green to yellow. However, reverse

oxidation did not regenerate the original absorption of **18**. When the visible spectra of **20** were measured under electrochemical reduction conditions, absorption band of **20** in the visible region at around 650 nm gradually decreased. Reverse oxidation of the reduced species decreased the new absorption bands, but did not regenerate the absorption band of **20**, completely. The greenish-blue color of the solution of **22** changed to yellow during electrochemical reduction, and reverse oxidation of the yellow-colored solution regenerated the visible spectra of **22**.

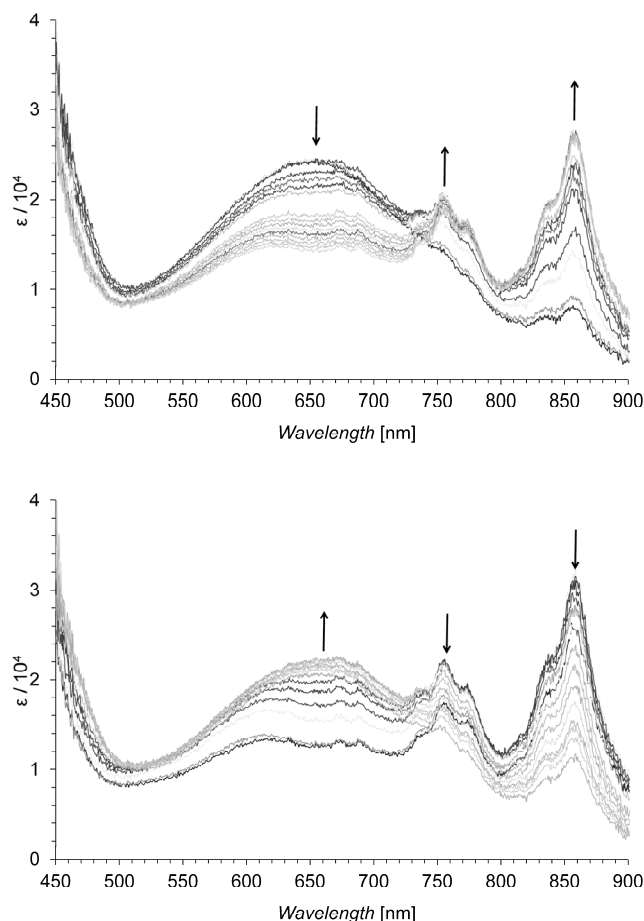
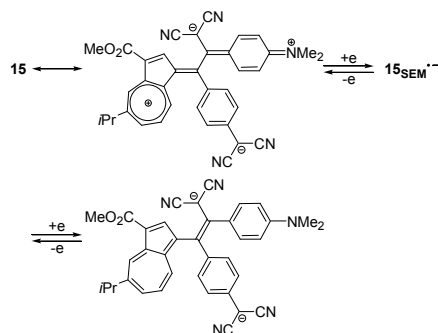


Figure 8. Continuous change in the UV–visible spectrum of **15**: constant-current electrochemical reduction (100 μA , top) and reverse oxidation of the reduced species (100 μA , bottom) in benzonitrile containing Et_4NClO_4 (0.1 M) at 30 sec intervals.



Scheme 10. Presumed redox behavior of DCNQ **15** (SEM is the semiquinone state formed by the single-electron transfer).

Conclusions

Several arylamine derivatives connected with multiple 1-azulenylethynyl groups **10–14** were prepared by Sonogashira–Hagihara cross-coupling reaction. A series of TCBD and DCNQ chromophores substituted by the 1-azulenyl groups were synthesized in a one-pot reaction consisting of the formal [2 + 2] cycloaddition reaction of **10–14** with TCNE and TCNQ, followed by the ring-opening reaction of the initially formed cyclobutene derivatives. Strong intramolecular CT absorption bands were observed in the UV/Vis spectra of these azulene-substituted TCBD and DCNQ derivatives. An analysis by CV and DPV showed that chromophores **14–21** exhibit a reversible two- or three stage reduction waves. Moreover, a significant color change was observed during the electrochemical reduction. In particular, DCNQ **15** exhibited a significant color change, arising from the generation of a stable dianionic structure during the electrochemical reduction.

Experimental Section

General: Melting points were determined with a Yanagimoto MPS3 micro melting apparatus and are uncorrected. Mass spectra were obtained with Bruker APEX II instruments. IR and UV/Vis spectra were measured with JASCO FT/IR-4100 and Shimadzu UV-2550 spectrophotometers, respectively. ¹H and ¹³C NMR spectra were recorded with a JEOL ECA-500 spectrometer (at 500 MHz and 125 MHz, respectively). Voltammetry measurements were carried out with a BAS 100B/W electrochemical workstation equipped with Pt working and auxiliary electrodes and a reference electrode formed from Ag/AgNO₃ (0.01 M) in acetonitrile containing tetrabutylammonium perchlorate (0.1 M). Elemental analyses were performed at the Research and Analytical Center for Giant Molecules, Graduate School of Science, Tohoku University.

Compound 10: To a solution of **9** (252 mg, 1.00 mmol), **5** (272 mg, 1.10 mmol), and CuI (19 mg, 0.10 mmol) in triethylamine (10 mL) and THF (10 mL) was added tetrakis(triphenylphosphine)palladium(0) (58 mg, 0.05 mmol). The resulting mixture was stirred at room temperature for 1 h under an Ar atmosphere. The reaction mixture was poured into a 10% NH₄Cl solution and extracted with CH₂Cl₂. The organic layer was washed with brine, dried over Na₂SO₄, and concentrated under reduced pressure. The residue was purified by column chromatography on silica gel with CH₂Cl₂ to give **10** (368 mg, 99%) as green crystals. M.p. 154.0–158.0 °C (CH₂Cl₂); IR (KBr disk): ν_{\max} = 2961 (w), 2197 (w), 1692 (m), 1602 (m), 1527 (m), 1444 (s), 1367 (m), 1235 (s), 1203 (s), 1122 (w), 1071 (w), 1040 (w), 951 (w), 881 (w), 809 (m), 783 (w) cm⁻¹; UV/Vis (CH₂Cl₂): λ_{\max} (log ϵ) = 248 (4.36), 300 (4.64), 332 sh (4.54), 409 (4.06), 440 sh (3.91), 589 (2.81) nm; ¹H NMR (500 MHz, CDCl₃): δ_{H} = 9.68 (d, 1H, J = 2.0 Hz, 4-H), 8.64 (d, 1H, J = 10.0 Hz, 8-H), 8.42 (s, 1H, 2-H), 7.76 (d, 1H, J = 10.0 Hz, 6-H), 7.47 (d, 2H, J = 9.0 Hz, 2',6'-H), 7.45 (t, 1H, J = 10.0 Hz, 7-H), 6.69 (d, 2H, J = 9.0 Hz, 3',5'-H), 3.95 (s, 3H, CO₂Me), 3.21 (sept, 2H, J = 6.5 Hz, *i*Pr), 3.00 (s, 6H, NMe₂), 1.42 (d, 6H, J = 6.5 Hz, *i*Pr) ppm; ¹³C NMR (125 MHz, CDCl₃): δ_{C} = 165.68 (CO₂Me), 150.08 (C-1'), 150.01 (C-5), 144.54 (C-3a), 142.44 (C-2), 141.13 (C-8a), 139.16 (C-6), 138.11 (C-4), 136.39 (C-8), 132.61 (C-2',6'), 127.13 (C-7), 114.88 (C-3), 112.05 (C-3',5'), 110.82 (C-4'), 110.31 (C-1), 94.69 (C≡C), 82.44 (C≡C), 51.24 (CO₂Me), 40.40 (NMe₂), 39.33 (*i*Pr), 24.73 (*i*Pr) ppm; HRMS (FAB) calcd for C₂₅H₂₅NO₂ [M]⁺ 371.1880, found 371.1885; Anal. Calcd for C₂₅H₂₅NO₂ (371.47): C, 80.83; H, 6.78; N, 3.77. found: C, 80.69; H, 6.79; N 3.61.

Compound 11: To a solution of **9** (555 mg, 2.20 mmol), **6** (421 mg, 1.00 mmol), and CuI (38 mg, 0.20 mmol) in triethylamine (15 mL) and THF (15 mL) was added tetrakis(triphenylphosphine)palladium(0) (116 mg, 0.10 mmol). The resulting mixture was stirred at 50 °C for 3 h under an Ar atmosphere. The reaction mixture was poured into a 10% NH₄Cl solution

and extracted with CH₂Cl₂. The organic layer was washed with brine, dried over Na₂SO₄, and concentrated under reduced pressure. The residue was purified by column chromatography on silica gel with CH₂Cl₂ to give **11** (630 mg, 94%) as green crystals. M.p. 110.0–114.0 °C (CH₂Cl₂); IR (KBr disk): ν_{\max} = 3348 (w), 2957 (w), 2196 (w), 1687 (s), 1597 (m), 1508 (s), 1447 (s), 1321 (m), 1241 (m), 1206 (s), 1124 (w), 1043 (w), 961 (w), 925 (w), 877 (w), 818 (m), 765 (m) cm⁻¹; UV/Vis (CH₂Cl₂): λ_{\max} (log ϵ) = 246 (4.69), 276 sh (4.57), 302 (4.76), 312 sh (4.75), 358 (4.76), 407 (4.54), 434 sh (4.42), 580 (3.11) nm; ¹H NMR (500 MHz, CDCl₃): δ_{H} = 9.72 (d, 2H, J = 1.5 Hz, 4-H), 8.65 (d, 2H, J = 10.0 Hz, 8-H), 8.46 (s, 2H, 2-H), 7.79 (d, 2H, J = 10.0 Hz, 6-H), 7.53 (d, 4H, J = 8.5 Hz, 2',2'',6',6''-H), 7.49 (t, 2H, J = 10.0 Hz, 7-H), 7.10 (d, 2H, J = 8.5 Hz, 3',3'',5',5''-H), 5.99 (s, 1H, NH), 3.96 (s, 6H, CO₂Me), 3.22 (sept, 2H, J = 6.5 Hz, *i*Pr), 1.42 (d, 12H, J = 6.5 Hz, *i*Pr) ppm; ¹³C NMR (125 MHz, CDCl₃): δ_{C} = 165.52 (CO₂Me), 150.34 (C-5), 144.63 (C-3a or 8a), 142.53 (C-2), 142.01 (C-3a or 8a), 141.15 (C-1',1''), 139.23 (C-6), 138.19 (C-4), 136.23 (C-8), 132.68 (C-2',2'',6',6''), 127.27 (C-5), 117.54 (C-3',3'',5',5''), 116.27 (C-4',4''), 114.94 (C-3), 109.52 (C-1), 93.76 (C≡C), 83.64 (C≡C), 51.15 (CO₂Me), 39.20 (*i*Pr), 24.58 (*i*Pr) ppm; HRMS (FAB) calcd for C₄₆H₃₉NO₄ [M]⁺ 669.2874, found 669.2872; Anal. Calcd for C₄₆H₃₉NO₄·1/2H₂O (669.81): C, 81.39; H, 5.94; N, 2.06. found: C, 81.41; H, 5.94; N, 2.05.

Compound 12: To a solution of **9** (555 mg, 2.20 mmol), **7** (419 mg, 1.00 mmol), and CuI (38 mg, 0.20 mmol) in triethylamine (15 mL) and THF (15 mL) was added tetrakis(triphenylphosphine)palladium(0) (116 mg, 0.10 mmol). The resulting mixture was stirred at 50 °C for 5 h under an Ar atmosphere. The reaction mixture was poured into a 10% NH₄Cl solution and extracted with CH₂Cl₂. The organic layer was washed with brine, dried over Na₂SO₄, and concentrated under reduced pressure. The residue was purified by column chromatography on silica gel with CH₂Cl₂ to give **12** (568 mg, 85%) as green crystals. M.p. 135.0–139.0 °C (CH₂Cl₂); IR (KBr disk): ν_{\max} = 3348 (w), 2956 (w), 2874 (w), 2196 (w), 1686 (s), 1603 (w), 1477 (s), 1446 (s), 1278 (w), 1245 (m), 1214 (s), 1169 (m), 1125 (m), 1043 (w), 877 (w), 807 (m), 767 (m) cm⁻¹; UV/Vis (CH₂Cl₂): λ_{\max} (log ϵ) = 249 (4.84), 282 sh (4.79), 305 sh (4.89), 316 (4.90), 406 (4.42), 425 sh (4.33), 581 (3.11) nm; ¹H NMR (500 MHz, CDCl₃): δ_{H} = 9.72 (d, 2H, J = 2.0 Hz, 4-H), 8.73 (d, 2H, J = 10.0 Hz, 8-H), 8.50 (s, 2H, 2-H), 8.35 (s, 2H, 4',5'-H), 8.32 (s, 1H, NH), 7.80 (d, 2H, J = 10.0 Hz, 6-H), 7.68 (d, 2H, J = 8.5 Hz, 2',7'-H), 7.52 (t, 2H, J = 10.0 Hz, 7-H), 7.42 (d, 2H, J = 8.5 Hz, 1',8'-H), 3.97 (s, 6H, CO₂Me), 3.23 (sept, 2H, J = 6.5 Hz, *i*Pr), 1.43 (d, 12H, J = 6.5 Hz, *i*Pr) ppm; ¹³C NMR (125 MHz, CDCl₃): δ_{C} = 165.59 (CO₂Me), 150.32 (C-5), 144.71 (C-3a), 142.56 (C-2), 141.17 (C-8a), 139.24 (C-6), 138.19 (C-4), 136.31 (C-8), 129.80 (C-2',7'), 127.30 (C-7), 123.84 (C-2), 123.10 (C-4a',4b'), 115.20 (C-8a',9a'), 114.93 (C-3), 110.90 (C-1',8'), 109.68 (C-1), 94.58 (C≡C), 83.04 (C≡C), 51.17 (CO₂Me), 39.22 (*i*Pr), 24.60 (*i*Pr) ppm; HRMS (FAB) calcd for C₄₆H₃₇NO₄ [M]⁺ 667.2718, found 667.2703; Anal. Calcd for C₄₆H₃₇NO₄·1/2H₂O (667.79): C, 81.63; H, 5.66; N, 2.07. found: C, 81.60; H, 5.64; N, 2.05.

Compound 13: To a solution of **9** (833 mg, 3.30 mmol), **8** (623 mg, 1.00 mmol), and CuI (57 mg, 0.30 mmol) in triethylamine (15 mL) and THF (15 mL) was added tetrakis(triphenylphosphine)palladium(0) (173 mg, 0.15 mmol). The resulting mixture was stirred at 50 °C for 6 h under an Ar atmosphere. The reaction mixture was poured into a 10% NH₄Cl solution and extracted with CH₂Cl₂. The organic layer was washed with brine, dried over Na₂SO₄, and concentrated under reduced pressure. The residue was purified by column chromatography on silica gel with CH₂Cl₂ to give **13** (897 mg, 90%) as green crystals. M.p. 131.0–133.0 °C (CHCl₃/MeOH); IR (KBr disk): ν_{\max} = 2957 (w), 2196 (w), 1693 (s), 1593 (w), 1496 (s), 1446 (s), 1381 (w), 1317 (m), 1280 (m), 1245 (m), 1204 (s), 1123 (m), 1044 (w), 958 (w), 919 (w), 877 (w), 831 (m), 776 (m), 726 (w) cm⁻¹; UV/Vis (CH₂Cl₂): λ_{\max} (log ϵ) = 247 (4.88), 306 (4.93), 370 (4.86), 408 (4.77), 433 sh (4.68), 576 (3.32) nm; ¹H NMR (500 MHz, CDCl₃): δ_{H} = 9.72 (d, 3H, J

= 1.5 Hz, 4-H), 8.65 (d, 3H, J = 10.0 Hz, 8-H), 8.46 (s, 3H, 2-H), 7.80 (d, 3H, J = 10.0 Hz, 6-H), 7.52 (d, 6H, J = 8.5 Hz, 3',5'-H), 7.50 (dd, 3H, J = 10.0, 10.0 Hz, 7-H), 7.14 (d, 6H, J = 8.5 Hz, 2',6'-H), 3.96 (s, 9H, CO₂Me), 3.24 (sept, 3H, J = 7.0 Hz, *i*Pr), 1.48 (d, 18H, J = 7.0 Hz, *i*Pr) ppm; ¹³C NMR (125 MHz, CDCl₃): δ_C = 165.45 (CO₂Me), 150.47 (C-5), 146.38 (C-1'), 144.69 (C-3a), 142.60 (C-2), 141.19 (C-8a), 139.28 (C-6), 138.25 (C-4), 136.20 (C-8), 132.51 (C-3',5'), 127.37 (C-7), 124.07 (C-2',6'), 118.51 (C-4'), 114.99 (C-3), 109.24 (C-1), 93.49 (C=C), 84.63 (C=C), 51.18 (CO₂Me), 39.24 (*i*Pr), 24.61 (*i*Pr) ppm; HRMS (FAB) calcd for C₆₉H₅₇NO₆⁺ [M]⁺ 995.4181, found 995.4185; Anal. Calcd for C₆₉H₅₇NO₆·1/10CHCl₃ (996.19): C, 82.32; H, 5.71; N, 1.39. found: C, 82.27; H, 5.81; N 1.41.

Compound 14: To a solution of **10** (186 mg, 0.50 mmol) in ethyl acetate (5 mL) was added TCNE (77 mg, 0.60 mmol). The resulting mixture was refluxed for 1 h under an Ar atmosphere. The solvent was removed under reduced pressure. The residue was purified by column chromatography on silica gel with CH₂Cl₂/ethyl acetate (20:1) to give **14** (242 mg, 97%) as red crystals. M.p. 159.0–162.0 °C (CH₂Cl₂/hexane); IR (KBr disk): ν_{max} = 2955 (w), 2213 (m), 1701 (m), 1603 (s), 1488 (s), 1438 (s), 1418 (m), 1383 (m), 1336 (m), 1295 (w), 1241 (w), 1210 (s), 1174 (s), 1055 (w), 943 (w), 902 (w), 814 (w), 779 (w), 735 (w) cm⁻¹; UV/Vis (CH₂Cl₂): λ_{max} (log ε) = 250 (4.44), 265 sh (4.42), 303 (4.65), 346 sh (4.17), 391 sh (4.24), 474 (4.49) nm; UV/Vis (20% CH₂Cl₂/hexane): λ_{max} (log ε) = 246 (4.44), 265 sh (4.43), 300 (4.38), 346 sh (4.19), 389 (4.25), 459 (4.49) nm; ¹H NMR (500 MHz, CDCl₃): δ_H = 9.97 (d, 1H, J = 2.0 Hz, 4-H), 8.51 (d, 1H, J = 10.0 Hz, 8-H), 8.31 (s, 1H, 2-H), 8.11 (d, 1H, J = 10.0 Hz, 6-H), 7.93 (dd, 1H, J = 10.0, 10.0 Hz, 7-H), 7.92 (d, 2H, J = 9.0 Hz, 2',6'-H), 6.78 (d, 2H, J = 9.0 Hz, 3',5'-H), 3.93 (s, 3H, CO₂Me), 3.34 (sept, 1H, J = 7.0 Hz, *i*Pr), 3.19 (s, 6H, NMe₂), 1.47 (d, 6H, J = 7.0 Hz, *i*Pr) ppm; ¹³C NMR (125 MHz, CDCl₃): δ_C = 165.54 (CO₂Me), 164.57 (C=C(CN)₂), 162.92 (C=C(CN)₂), 156.34 (C-5), 154.36 (C-1'), 145.98 (C-8a), 142.93 (C-2), 142.09 (C-6), 141.87 (C-3a), 140.36 (C-4), 137.71 (C-8), 132.82 (C-2',6'), 131.95 (C-7), 120.07 (C-1), 119.18 (C-3), 118.94 (C-4'), 114.64 (CN), 114.07 (CN), 113.53 (CN), 112.66 (CN), 112.24 (C-3',5'), 80.54 (C(CN)₂), 74.85 (C(CN)₂), 51.59 (CO₂Me), 40.18 (NMe₂), 39.43 (*i*Pr), 24.49 (*i*Pr) ppm; HRMS (FAB) calcd for C₃₁H₂₅N₅O₂⁺ [M]⁺ 499.2003, found 499.2006; Anal. Calcd for C₃₁H₂₅N₅O₂ (499.56): C, 74.53; H, 5.04; N, 14.02. found: C, 74.39; H, 4.88; N 13.98.

Reaction of 10 with TCNQ: To a solution of **10** (186 mg, 0.50 mmol) in ethyl acetate (10 mL) was added TCNQ (123 mg, 0.60 mmol). The resulting mixture was refluxed for 12 h under an Ar atmosphere. The solvent was removed under reduced pressure. The residue was purified by column chromatography on silica gel with CH₂Cl₂/ethyl acetate (10:1) to give **15** (124 mg, 43%) as dark green crystals and **16** (138 mg, 48%) as dark green crystals, respectively.

Compound 15: M.p. 181.0–184.0 °C (CH₂Cl₂/hexane); IR (KBr disk): ν_{max} = 2960 (w), 2927 (w), 2207 (m), 1698 (m), 1602 (s), 1540 (w), 1490 (m), 1438 (s), 1420 (m), 1379 (s), 1330 (m), 1288 (w), 1210 (s), 1189 (s), 1172 (s), 1130 (w), 1087 (w), 1046 (w), 998 (w), 972 (w), 943 (w), 903 (w), 860 (w), 838 (w), 820 (w), 780 (w), 700 (w), 670 (w) cm⁻¹; UV/Vis (CH₂Cl₂): λ_{max} (log ε) = 243 (4.45), 298 (4.41), 377 sh (4.72), 401 (4.92), 453 sh (4.35), 631 (4.37) nm; UV/Vis (10% CH₂Cl₂/hexane): λ_{max} (log ε) = 242 (4.45), 297 (4.41), 374 (4.75), 393 (4.97), 593 (4.36) nm; ¹H NMR (500 MHz, CDCl₃): δ_H = 9.88 (d, 1H, J = 1.5 Hz, 4-H), 8.38 (d, 1H, J = 10.0 Hz, 8-H), 8.18 (s, 1H, 2-H), 7.97 (d, 1H, J = 10.0 Hz, 6-H), 7.79 (d, 2H, J = 9.5 Hz, 2',6'-H), 7.65 (dd, 1H, J = 10.0, 10.0 Hz, 7-H), 7.15–7.05 (m, 4H, H_{DCNQ}), 6.67 (d, 2H, J = 9.5 Hz, 3',5'-H), 3.94 (s, 3H, CO₂Me), 3.30 (sept, 1H, J = 7.0 Hz, *i*Pr), 3.13 (s, 6H, NMe₂), 1.45 (d, 6H, J = 7.0 Hz, *i*Pr) ppm; ¹³C NMR (125 MHz, CDCl₃): δ_C = 169.29 (C_{DCNQ}), 164.79 (CO₂Me), 154.58 (C-5), 154.27 (C=C(CN)₂), 153.87 (C=C(CN)₂), 148.25 (C-1'),

144.96 (C-8a), 143.73 (C-3a), 143.67 (C-2), 141.43 (C-6), 139.99 (C-4), 136.69 (C-8), 136.29 (C_{DCNQ}), 134.55 (C_{DCNQ}), 132.79 (C-2',6'), 132.57, 130.94 (C-7), 125.09 (C_{DCNQ}), 124.95 (C-1), 124.60 (C_{DCNQ}), 121.54 (C-4'), 118.79 (C-3), 115.26 (CN), 114.48 (CN), 114.39 (CN), 114.26 (CN), 111.93 (C-3',5'), 76.38 (C(CN)₂), 73.01 (C(CN)₂), 51.51 (CO₂Me), 40.10 (NMe₂), 39.34 (*i*Pr), 24.49 (*i*Pr) ppm; HRMS (FAB) calcd for C₃₇H₂₉N₅O₂⁺ [M]⁺ 575.2316, found 575.2340; Anal. Calcd for C₃₇H₂₉N₅O₂ (575.66): C, 77.20; H, 5.08; N, 12.17. found: C, 77.08; H, 5.19; N 12.13.

Compound 16: M.p. 183.0–187.0 °C decomp. (CH₂Cl₂/hexane); IR (KBr disk): ν_{max} = 2956 (w), 2202 (m), 1697 (m), 1581 (s), 1485 (w), 1440 (m), 1417 (m), 1367 (s), 1347 (s), 1325 (w), 1273 (w), 1231 (w), 1221 (w), 1169 (s), 1130 (w), 1048 (w), 998 (w), 942 (w), 908 (w), 838 (w), 818 (w), 793 (w), 746 (w), 725 (w), 674 (w) cm⁻¹; UV/Vis (CH₂Cl₂): λ_{max} (log ε) = 238 (4.46), 262 (4.42), 301 (4.45), 338 (4.38), 415 (4.43), 462 sh (4.30), 689 (4.52) nm; UV/Vis (10% CH₂Cl₂/hexane): λ_{max} (log ε) = 262 (4.43), 301 (4.43), 334 (4.39), 409 (4.44), 619 (4.48) nm; ¹H NMR (500 MHz, CDCl₃): δ_H = 9.93 (d, 1H, J = 1.5 Hz, 4-H), 8.57 (s, 1H, 2-H), 8.45 (d, 1H, J = 10.0 Hz, 8-H), 8.02 (d, 1H, J = 10.0 Hz, 6-H), 7.76 (dd, 1H, J = 10.0, 10.0 Hz, 7-H), 7.51 (dd, 1H, J = 9.5, 2.0 Hz, H_{DCNQ}), 7.36 (d, 2H, J = 9.0 Hz, 2',6'-H), 7.24 (dd, 1H, J = 9.5, 2.0 Hz, H_{DCNQ}), 7.02 (dd, 1H, J = 9.5, 2.0 Hz, H_{DCNQ}), 6.98 (dd, 1H, J = 9.5, 2.0 Hz, H_{DCNQ}), 6.70 (d, 2H, J = 9.0 Hz, 3',5'-H), 3.93 (s, 3H, CO₂Me), 3.30 (sept, 1H, J = 7.0 Hz, *i*Pr), 3.12 (s, 6H, NMe₂), 1.44 (d, 6H, J = 7.0 Hz, *i*Pr) ppm; ¹³C NMR (125 MHz, CDCl₃): δ_C = 166.28, 164.63 (CO₂Me), 155.62, 154.09, 153.97, 152.86, 145.55, 143.25, 141.67, 141.57, 140.20, 136.43, 136.07, 134.99, 134.45, 132.78, 132.62, 131.22, 125.14, 125.02, 124.49, 122.84, 118.47, 114.95, 114.82 (CN), 113.53 (CN), 112.47 (CN), 111.91 (CN), 82.35 (C(CN)₂), 70.89 (C(CN)₂), 51.62 (CO₂Me), 40.18 (NMe₂), 39.33 (*i*Pr), 24.46 (*i*Pr) ppm; HRMS (FAB) calcd for C₃₇H₂₉N₅O₂⁺ [M]⁺ 575.2316, found 575.2313; Anal. Calcd for C₃₇H₂₉N₅O₂ (575.66): C, 77.20; H, 5.08; N, 12.17. found: C, 77.11; H, 5.16; N 12.15.

Compound 17: To a solution of **11** (201 mg, 0.30 mmol) in ethyl acetate (10 mL) was added TCNE (102 mg, 0.80 mmol). The resulting mixture was refluxed for 6 h under an Ar atmosphere. The solvent was removed under reduced pressure. The residue was purified by column chromatography on silica gel with CH₂Cl₂/ethyl acetate (20:1) to give **17** (272 mg, 98%) as red crystals. M.p. 170.0–172.0 °C (CH₂Cl₂/hexane); IR (KBr disk): ν_{max} = 2953 (w), 2224 (m), 1700 (m), 1588 (s), 1489 (s), 1439 (m), 1418 (m), 1383 (m), 1284 (w), 1240 (w), 1212 (w), 1179 (s), 1093 (w), 1041 (w), 902 (w), 817 (w), 777 (w), 729 (w), 664 (w) cm⁻¹; UV/Vis (CH₂Cl₂): λ_{max} (log ε) = 262 (4.80), 300 (4.74), 340 sh (4.57), 389 sh (4.48), 489 (4.81) nm; UV/Vis (20% CH₂Cl₂/hexane): λ_{max} (log ε) = 246 (4.44), 262 (4.43), 300 (4.38), 341 sh (4.21), 389 (4.25), 459 (4.49) nm; ¹H NMR (500 MHz, CDCl₃): δ_H = 10.00 (d, 2H, J = 2.0 Hz, 4-H), 8.49 (d, 2H, J = 10.0 Hz, 8-H), 8.30 (s, 2H, 2-H), 8.16 (d, 2H, J = 10.0 Hz, 6-H), 7.99 (d, 2H, J = 10.0 Hz, 7-H), 7.90 (d, 4H, J = 8.5 Hz, 2',6'-H), 7.32 (d, 4H, J = 8.5 Hz, 3',5'-H), 7.29 (s, 1H, NH), 3.95 (s, 6H, CO₂Me), 3.35 (sept, 2H, J = 7.0 Hz, *i*Pr), 1.47 (d, 12H, J = 7.0 Hz, *i*Pr) ppm; ¹³C NMR (125 MHz, CDCl₃): δ_C = 167.05 (C-1'), 164.41 (CO₂Me), 161.16 (C=C(CN)₂), 157.13 (C-5), 146.25 (C=C(CN)₂), 146.21 (C-8a), 142.61 (C-2 or 6), 142.58 (C-2 or 6), 142.00 (C-3a), 140.77 (C-4), 137.68 (C-8), 132.44 (C-2',6'), 132.38 (C-7), 125.86 (C-4'), 119.69 (C-1), 119.51 (C-3), 118.52 (C-3',5'), 113.75 (CN), 112.96 (CN), 112.66 (CN), 111.86 (CN), 83.19 (C(CN)₂), 80.33 (C(CN)₂), 51.76 (CO₂Me), 39.51 (*i*Pr), 24.49 (*i*Pr) ppm; HRMS (FAB) calcd for C₅₈H₃₉N₉O₄⁺ [M]⁺ 925.3120, found 925.3139; Anal. Calcd for C₅₈H₃₉N₉O₄ (925.99): C, 75.23; H, 4.25; N, 13.61. found: C, 75.10; H, 4.38; N 13.57.

Compound 18: To a solution of **11** (201 mg, 0.30 mmol) in ethyl acetate (15 mL) was added TCNQ (204 mg, 1.00 mmol). The resulting mixture was refluxed for 12 h under an Ar atmosphere. The solvent was removed under reduced pressure. The residue was purified by column chromatography on

silica gel with CH₂Cl₂/ethyl acetate (10:1) to give **18** (294 mg, 91%) as dark green crystals. M.p. 246.0–248.0 °C (CH₂Cl₂/hexane); IR (KBr disk): ν_{\max} = 2961 (w), 2208 (m), 1698 (m), 1588 (s), 1505 (s), 1439 (s), 1420 (m), 1398 (m), 1381 (m), 1350 (m), 1317 (m), 1279 (m), 1214 (s), 1189 (s), 1128 (w), 1085 (w), 1046 (w), 974 (w), 904 (w), 836 (w), 809 (w), 778 (w), 757 (w), 744 (w), 727 (w), 655 (w) cm⁻¹; UV/Vis (CH₂Cl₂): λ_{\max} (log ϵ) = 242 (4.79), 297 (4.80), 421 (4.76), 628 (4.71) nm; UV/Vis (50% CH₂Cl₂/hexane): λ_{\max} (log ϵ) = 242 (4.80), 297 (4.81), 417 (4.77), 617 (4.71) nm; ¹H NMR (500 MHz, CDCl₃): δ_{H} = 9.87 (d, 2H, J = 2.0 Hz, 4-H), 8.31 (d, 2H, J = 10.0 Hz, 8-H), 8.16 (s, 2H, 2-H), 8.00 (d, 2H, J = 10.0 Hz, 6-H), 7.75 (d, 4H, J = 9.0 Hz, 2',5'-H), 7.67 (dd, 2H, J = 10.0, 10.0 Hz, 7-H), 7.18–7.15 (m, 8H, H_{DCNQ} and 3',5'-H), 7.12–7.04 (m, 3H, H_{DCNQ} and NH), 3.94 (s, 6H, CO₂Me), 3.30 (sept, 2H, J = 7.0 Hz, *i*Pr), 1.45 (d, 12H, J = 7.0 Hz, *i*Pr) ppm; ¹³C NMR (125 MHz, CDCl₃): δ_{C} = 170.38 (C_{DCNQ}), 164.65 (CO₂Me), 155.01 (C-5), 153.86 (C=C(CN)₂), 146.21 (C=C(CN)₂), 145.71 (C-1'), 144.87 (C-8a), 143.78 (C-3a), 143.37 (C-2), 141.73 (C-6), 140.22 (C-4), 136.37 (C-8 or C_{DCNQ}), 136.27 (C-8 or C_{DCNQ}), 134.04 (C_{DCNQ}), 133.24, 132.18 (C-2',6'), 131.14 (C-7), 128.13 (C-4'), 125.57 (C_{DCNQ}), 125.10 (C_{DCNQ}), 124.47 (C-1), 119.02 (C-3), 118.13 (C-3',5'), 114.20 (CN×2), 113.80 (CN), 112.81 (CN), 83.35 (C(CN)₂), 74.07 (C(CN)₂), 51.63 (CO₂Me), 39.35 (*i*Pr), 24.46 (*i*Pr) ppm; HRMS (FAB) calcd for C₇₀H₄₇N₉O₄⁺ [M]⁺ 1077.3746, found 1077.3776; Anal. Calcd for C₇₀H₄₇N₉O₄·2/5H₂O (1078.18): C, 77.46; H, 4.44; N, 11.61. found: C, 77.52; H, 4.50; N 11.60.

Compound 19: To a solution of **12** (200 mg, 0.30 mmol) in ethyl acetate (10 mL) was added TCNE (102 mg, 0.80 mmol). The resulting mixture was refluxed for 6 h under an Ar atmosphere. The solvent was removed under reduced pressure. The residue was purified by column chromatography on silica gel with CH₂Cl₂/ethyl acetate (20:1) to give **19** (255 mg, 92%) as red crystals. M.p. 217.0–220.0 °C decomp. (CH₂Cl₂/hexane); IR (KBr disk): ν_{\max} = 2957 (w), 2875 (w), 2221 (m), 1700 (m), 1628 (w), 1600 (m), 1496 (s), 1442 (s), 1418 (s), 1363 (m), 1313 (w), 1280 (w), 1255 (m), 1236 (s), 1213 (s), 1179 (s), 1143 (s), 1087 (w), 1041 (w), 904 (w), 812 (m), 777 (m), 729 (w), 695 (w), 678 (w) cm⁻¹; UV/Vis (CH₂Cl₂): λ_{\max} (log ϵ) = 233 (4.78), 266 (4.77), 299 (4.80), 347 sh (4.55), 403 (4.50), 456 (4.58) nm; UV/Vis (20% CH₂Cl₂/hexane): λ_{\max} (log ϵ) = 233 (4.78), 263 (4.78), 299 (4.80), 347 sh (4.55), 402 (4.53), 449 (4.55) nm; ¹H NMR (500 MHz, CDCl₃): δ_{H} = 9.95 (d, 2H, J = 2.0 Hz, 4-H), 9.50 (s, 1H, NH), 8.61 (d, 2H, J = 1.5 Hz, 4',5'-H), 8.55 (d, 2H, J = 10.0 Hz, 8-H), 8.27 (s, 2H, 2-H), 8.14 (d, 2H, J = 10.0 Hz, 6-H), 8.00 (dd, 2H, J = 10.0, 10.0 Hz, 7-H), 7.84 (dd, 2H, J = 9.0, 1.5 Hz, 2',7'-H), 7.44 (d, 2H, J = 9.0 Hz, 1',8'-H), 3.89 (s, 6H, CO₂Me), 3.33 (sept, 2H, J = 7.0 Hz, *i*Pr), 1.44 (d, 12H, J = 7.0 Hz, *i*Pr) ppm; ¹³C NMR (125 MHz, CDCl₃): δ_{C} = 168.69 (C-3',6'), 164.43 (CO₂Me), 161.01 (C=C(CN)₂), 157.03 (C-5), 146.14 (C-8a), 143.39 (C-4a',4b'), 142.59 (C-2 or 6), 142.47 (C-2 or 6), 141.96 (C-3a), 140.72 (C-4), 137.71 (C-8), 132.47 (C-7), 129.42 (C-2',7'), 124.70 (C=C(CN)₂), 123.35 (C-8a',9a'), 123.22 (C-4',5'), 119.49 (C-1 or 3), 119.35 (C-1 or 3), 113.67 (CN), 113.46 (CN), 113.16 (CN), 112.99 (C-1',8'), 111.83 (CN), 84.27 (C(CN)₂), 81.08 (C(CN)₂), 51.74 (CO₂Me), 39.49 (*i*Pr), 24.47 (*i*Pr) ppm; HRMS (FAB) calcd for C₅₈H₃₇N₉O₄⁺ [M]⁺ 923.2964, found 923.2978; Anal. Calcd for C₅₈H₃₇N₉O₄ (923.97): C, 75.39; H, 4.04; N, 13.64. found: C, 75.18; H, 4.15; N 13.58.

Compound 20: To a solution of **12** (200 mg, 0.30 mmol) in ethyl acetate (15 mL) was added TCNE (204 mg, 1.00 mmol). The resulting mixture was refluxed for 12 h under an Ar atmosphere. The solvent was removed under reduced pressure. The residue was purified by column chromatography on silica gel with CH₂Cl₂/ethyl acetate (10:1) to give **20** (271 mg, 84%) as dark green crystals. M.p. 267.0–273.0 °C (CH₂Cl₂/hexane); IR (KBr disk): ν_{\max} = 2957 (w), 2208 (m), 1698 (m), 1599 (m), 1506 (s), 1442 (s), 1419 (s), 1397 (s), 1380 (m), 1358 (m), 1309 (w), 1270 (w), 1213 (s), 1191 (s), 1141 (w), 1087 (w), 1045 (w), 930 (w), 905 (w), 838 (w), 811 (w), 776 (w), 729 (w),

664 (w), 655 (w) cm⁻¹; UV/Vis (CH₂Cl₂): λ_{\max} (log ϵ) = 241 (4.88), 297 (4.91), 386 (4.73), 637 (4.70) nm; UV/Vis (50% CH₂Cl₂/hexane): λ_{\max} (log ϵ) = 240 (4.87), 297 (4.91), 382 (4.72), 626 (4.69) nm; ¹H NMR (500 MHz, CDCl₃): δ_{H} = 9.86 (d, 2H, J = 2.0 Hz, 4-H), 9.16 (s, 1H, NH), 8.57 (d, 2H, J = 1.5 Hz, 4',5'-H), 8.35 (d, 2H, J = 10.0 Hz, 8-H), 8.23 (s, 2H, 2-H), 7.98 (d, 2H, J = 10.0 Hz, 6-H), 7.74 (dd, 2H, J = 8.5, 1.5 Hz, 2',7'-H), 7.68 (dd, 2H, J = 10.0, 10.0 Hz, 7-H), 7.48 (s, 2H, J = 8.5 Hz, 1',8'-H), 7.18–7.13 (m, 4H, H_{DCNQ}), 7.10 (br s, 4H, H_{DCNQ}), 3.93 (s, 6H, CO₂Me), 3.28 (sept, 2H, J = 7.0 Hz, *i*Pr), 1.44 (d, 12H, J = 7.0 Hz, *i*Pr) ppm; ¹³C NMR (125 MHz, CDCl₃): δ_{C} = 172.23 (C_{DCNQ}), 164.68 (CO₂Me), 155.04 (C-5), 153.75 (C=C(CN)₂), 146.30 (C_{DCNQ}), 144.85 (C-8a), 143.86 (C=C(CN)₂), 143.52 (C-2), 142.91 (C-3a), 141.78 (C-6), 140.22 (C-4), 136.35 (C-8 and C_{DCNQ}), 134.09, 133.83 (C_{DCNQ}), 131.29 (C-7), 129.33 (C-2',7'), 127.73, 125.72, 125.19 (C_{DCNQ}), 124.69 (C_{DCNQ}), 123.54 (C-1), 123.18 (C-4',5'), 119.04 (C-3), 114.15 (CN×2), 113.97 (C-1',8' and CN), 112.69 (CN), 84.87 (C(CN)₂), 74.30 (C(CN)₂), 51.66 (CO₂Me), 39.36 (*i*Pr), 24.46 (*i*Pr) ppm; HRMS (FAB) calcd for C₇₀H₄₅N₉O₄⁺ [M]⁺ 1075.3590, found 1075.3605; Anal. Calcd for C₇₀H₄₅N₉O₄·3/4H₂O (1076.16): C, 77.16; H, 4.30; N, 11.57. found: C, 77.26; H, 4.41; N 11.56.

Compound 21: To a solution of **13** (199 mg, 0.20 mmol) in ethyl acetate (10 mL) was added TCNE (128 mg, 1.00 mmol). The resulting mixture was refluxed for 6 h under an Ar atmosphere. The solvent was removed under reduced pressure. The residue was purified by column chromatography on silica gel with CH₂Cl₂/ethyl acetate (10:1) to give **21** (249 mg, 90%) as red crystals. M.p. 201.0–205.0 °C decomp. (CH₂Cl₂/hexane); IR (KBr disk): ν_{\max} = 2962 (w), 2879 (w), 2221 (m), 1698 (m), 1590 (m), 1496 (s), 1441 (m), 1418 (m), 1363 (w), 1327 (w), 1291 (m), 1240 (w), 1212 (m), 1181 (s), 1134 (w), 1086 (w), 1053 (w), 906 (w), 812 (w), 778 (m), 732 (m), 712 (w), 668 (w) cm⁻¹; UV/Vis (CH₂Cl₂): λ_{\max} (log ϵ) = 264 (4.95), 300 (4.92), 338 sh (4.73), 404 (4.66), 503 (4.86) nm; UV/Vis (20% CH₂Cl₂/hexane): λ_{\max} (log ϵ) = 264 (4.94), 298 (4.91), 338 sh (4.71), 403 (4.64), 488 (4.84) nm; ¹H NMR (500 MHz, CDCl₃): δ_{H} = 10.01 (d, 3H, J = 2.0 Hz, 4-H), 8.47 (d, 3H, J = 10.0 Hz, 8-H), 8.29 (s, 3H, 2-H), 8.17 (d, 3H, J = 10.0 Hz, 6-H), 8.00 (dd, 3H, J = 10.0, 10.0 Hz, 7-H), 7.87 (d, 6H, J = 9.0 Hz, 2',6'-H), 7.39 (d, 6H, J = 9.0 Hz, 3',5'-H), 3.97 (s, 9H, CO₂Me), 3.36 (sept, 3H, J = 7.0 Hz, *i*Pr), 1.48 (d, 18H, J = 7.0 Hz, *i*Pr) ppm; ¹³C NMR (125 MHz, CDCl₃): δ_{C} = 167.07 (C=C(CN)₂), 164.31 (CO₂Me), 160.38 (C=C(CN)₂), 157.31 (C-5), 149.80 (C-1'), 146.24 (C-8a), 142.72 (C-6), 142.45 (C-2), 141.98 (C-3a), 140.91 (C-4), 137.63 (C-8), 132.45 (C-7), 132.16 (C-2',6'), 128.80 (C-4'), 125.26 (C-3',5'), 119.70 (C-1), 119.50 (C-3), 113.61 (CN), 112.56 (CN), 112.37 (CN), 111.33 (CN), 86.17 (C(CN)₂), 80.53 (C(CN)₂), 51.81 (CO₂Me), 39.53 (*i*Pr), 24.48 (*i*Pr) ppm; HRMS (FAB) calcd for C₈₇H₅₇N₁₃O₆⁺ [M]⁺ 1379.4550, found 1379.4575; Anal. Calcd for C₈₇H₅₇N₁₃O₆·3/4H₂O (1380.47): C, 74.96; H, 4.23; N, 13.06. found: C, 75.11; H, 4.41; N, 13.05.

Compound 22: To a solution of **13** (199 mg, 0.20 mmol) in ethyl acetate (20 mL) was added TCNE (204 mg, 1.00 mmol). The resulting mixture was refluxed for 24 h under an Ar atmosphere. The solvent was removed under reduced pressure. The residue was purified by column chromatography on silica gel with CH₂Cl₂/ethyl acetate (10:1) to give **22** (280 mg, 87%) as dark green crystals. M.p. 264.0–267.0 °C decomp. (CH₂Cl₂/hexane); IR (KBr disk): ν_{\max} = 2959 (w), 2209 (m), 1697 (m), 1591 (m), 1503 (s), 1440 (s), 1420 (s), 1383 (m), 1330 (m), 1279 (m), 1212 (s), 1191 (s), 1128 (w), 1086 (w), 1032 (w), 972 (w), 904 (w), 839 (w), 809 (w), 777 (w), 729 (w), 698 (w), 673 (w), 657 (w) cm⁻¹; UV/Vis (CH₂Cl₂): λ_{\max} (log ϵ) = 243 (5.01), 296 (5.05), 394 sh (4.83), 422 (4.89), 628 (4.85) nm; UV/Vis (50% CH₂Cl₂/hexane): λ_{\max} (log ϵ) = 243 (4.99), 296 (5.02), 394 sh (4.83), 419 (4.89), 617 (4.83) nm; ¹H NMR (500 MHz, CDCl₃): δ_{H} = 9.88 (d, 3H, J = 1.5 Hz, 4-H), 8.28 (d, 3H, J = 10.0 Hz, 8-H), 8.15 (s, 3H, 2-H), 8.02 (d, 3H, J = 10.0 Hz, 6-H), 7.72 (d, 6H, J = 8.0 Hz, 2',6'-H), 7.67 (dd, 1H, J = 10.0, 10.0 Hz, 7-H), 7.19–7.13 (m, 12H, H_{DCNQ} and 3',5'-H), 7.07–7.01 (m, 6H,

H_{DCNQ} , 3.96 (s, 9H, CO₂Me), 3.31 (sept, 1H, $J = 7.0$ Hz, *i*Pr), 1.47 (d, 18H, $J = 7.0$ Hz, *i*Pr) ppm; ¹³C NMR (125 MHz, CDCl₃): $\delta_c = 170.23$ (C_{DCNQ}), 164.64 (CO₂Me), 155.10 (C-5), 153.62 (C=C(CN)₂), 149.25 (C-1'), 145.13 (C=C(CN)₂), 144.75 (C-8a), 143.82 (C-3a), 143.05 (C-2), 141.87 (C-6), 140.29 (C-4), 136.37 (C-8), 136.15 (C_{DCNQ}), 133.68 (C_{DCNQ}), 133.25 (C-4'), 131.78 (C-2',6'), 131.19 (C-7), 131.01, 125.78 (C_{DCNQ}), 125.32 (C_{DCNQ}), 124.84 (C-3',5'), 124.17 (C-1), 119.13 (C-3), 114.07 (CN), 113.96 (CN), 113.24 (CN), 112.27 (CN), 85.93 (C(CN)₂), 74.94 (C(CN)₂), 51.72 (CO₂Me), 39.38 (*i*Pr), 24.48 (*i*Pr) ppm; HRMS (FAB) calcd for C₁₀₅H₆₉N₁₃O₆⁺ [M]⁺ 1607.5489, found 1607.5481; Anal. Calcd for C₁₀₅H₆₉N₁₃O₆·H₂O (1608.76): C, 77.52; H, 4.40; N, 11.19. found: C, 77.65; H, 4.52; N 11.12.

Supporting Information (see footnote on the first page of this article): Copies of ¹H and ¹³C NMR, UV/Vis spectra and continuous change in the visible spectra of the reported compounds.

Acknowledgments

This work was partially supported by a Grant-in-Aid for Research (Grant 22850007 and 25810019 to T.S.) from the Ministry of Education, Culture, Sports, Science, and Technology, Japan.

- [1] a) J. Kido, Y. Okamoto, *Chem. Rev.* **2002**, *102*, 2357–2368; b) A. C. Grimsdale, K. L. Chan, R. E. Martin, P. G. Jokisz, A. B. Holmes, *Chem. Rev.* **2009**, *109*, 897–1091; c) M. Zhu, J. Zou, X. He, C. Yang, H. Wu, C. Zhong, J. Qin, Y. Cao, *Chem. Mater.* **2012**, *24*, 174–180; d) Y. Zhang, S.-L. Lai, Q.-X. Tong, M.-F. Lo, T.-W. Ng, M.-Y. Chan, Z.-C. Wen, J. He, K.-S. Jeff, X.-L. Tang, W.-M. Liu, C.-C. Ko, P.-F. Wang, C.-S. Lee, *Chem. Mater.* **2012**, *24*, 61–70; e) Y. Liu, S. Chen, J. W. Y. Lam, P. Lu, R. T. K. Kwok, F. Mahtab, H. S. Kwok, B. Z. Tang, *Chem. Mater.* **2011**, *23*, 2536–2544.
- [2] a) J. Rivnay, S. C. B. Mannsfeld, C. E. Miller, A. Salleo, M. F. Toney, *Chem. Rev.* **2012**, *112*, 5488–5519; b) S. Feser, K. Meerholz, *Chem. Mater.* **2011**, *23*, 5001–5005.
- [3] a) S.-C. Lo, P. L. Burn, *Chem. Rev.* **2007**, *107*, 1097–1116; b) Y.-J. Cheng, S.-H. Yang, C.-S. Hsu, *Chem. Rev.* **2009**, *109*, 5868–5923; c) X. Ren, S. Jiang, M. Cha, G. Zhou, Z.-S. Wang, *Chem. Mater.* **2012**, *24*, 3493–3499; d) W. Z. Yuan, Y. Gong, S. Chen, X. Y. Shen, J. W. Y. Lam, P. Lu, Y. Lu, Z. Wang, R. Hu, N. Xie, H. S. Kwok, Y. Zhang, J. Z. Sun, B. Z. Tang, *Chem. Mater.* **2012**, *24*, 1518–1528; e) Y. Sun, S.-C. Chien, H.-L. Yip, Y. Zhang, K.-S. Chen, D. F. Zeigler, F.-C. Chen, B. Lin, A. K.-Y. Jen, *Chem. Mater.* **2011**, *23*, 5006–5015.
- [4] a) X.-D. Zhuang, Y. Chen, B.-X. Li, D.-G. Ma, B. Zhang, Y. Li, *Chem. Mater.* **2010**, *22*, 4455–4461; b) W.-Y. Lee, T. Kurosawa, S.-T. Lin, T. Higashihara, M. Ueda, W.-C. Chen, *Chem. Mater.* **2011**, *23*, 4487–4497; c) Q.-D. Ling, D.-J. Liaw, C. Zhu, D. S.-H. Chan, E.-T. Kang, K.-G. Neoh, *Prog. Polym. Sci.* **2008**, *33*, 917–978; d) K.-L. Wang, Y.-L. Liu, I.-H. Shin, K.-G. Neoh, E.-T. Kang, *J. Polym. Sci., Part A Polym. Chem.* **2010**, *48*, 5790–5800; e) K.-L. Wang, Y.-L. Liu, J.-W. Lee, K.-G. Neoh, E.-T. Kang, *Macromolecules* **2010**, *43*, 7159–7164.
- [5] a) A. Leliege, P. Blanchard, T. Rousseau, J. Roncali, *Org. Lett.*, **2011**, *13*, 3098–3101; b) J. Wu, J. Liu, T. Zhou, S. Bo, L. Qiu, Z. Zhen, X. Liu, *RSC Adv.* **2012**, *2*, 1416–1423; c) A. R. Morales, A. Frazer, A. W. Woodward, H.-Y. Ahn-White, A. Fonari, P. Tongwa, T. Timofeeva, K. D. Belfield, *J. Org. Chem.* **2013**, *78*, 1014–1025.
- [6] a) S. Kato, F. Diederich, *Chem. Commun.* **2010**, *46*, 1994–2006; b) M. Kivala, F. Diederich, *Acc. Chem. Res.* **2009**, *42*, 235–248; c) M. Kivala, T. Stanoeva, T. Michinobu, B. Frank, G. Gescheidt, F. Diederich, *Chem. Eur. J.* **2008**, *14*, 7638–7647; d) B. B. Frank, B. C. Blanco, S. Jakob, F. Ferroni, S. Pieraccini, A. Ferrarini, C. Boudon, J.-P. Gisselbrecht, P. Seiler, G. P. Spada, F. Diederich, *Chem. Eur. J.* **2009**, *15*, 9005–9016; e) P. Fesser, C. Iacovita, C. Wäckerlin, S. Vijayaraghavan, N. Ballav, K. Howes, J.-P. Gisselbrecht, M. Croub, C. Boudon, M. Stchr, T. A. Jung, F. Diederich, *Chem. Eur. J.* **2011**, *17*, 5246–5250; f) B. Breiten, Y.-L. Wu, P. D. Jarowski, J.-P. Gisselbrecht, C. Boudon, M. Griesser, C. Onitsch, G. Gescheidt, W. B. Schweizer, N. Langer, C. Lennartz, F. Diederich, *Chem. Sci.*, **2011**, *2*, 88–93; g) A. R. Lacy, A. Vogt, C. Boudon, J.-P. Gisselbrecht, W. B. Schweizer, F. Diederich, *Eur. J. Org. Chem.*, **2013**, 869–879; h) B. H. Tchitchanov, M. Chiu, M. Jordan, M. Kivala, W. B. Schweizer, F. Diederich, *Eur. J. Org. Chem.*, **2013**, 3729–3740.
- [7] a) T. Michinobu, *Chem. Soc. Rev.* **2011**, *40*, 2306–2316; b) Y. Yuan, T. Michinobu, *J. Polym. Sci. Part A Polym. Chem.*, **2011**, *49*, 225–233; c) H. Fujita, K. Tsuboi, T. Michinobu, *Macromol. Chem. Phys.* **2011**, *212*, 1758–1766; d) Y. Washino, T. Michinobu, *Macromol. Rapid Commun.* **2011**, *32*, 644–648; e) Y. Li, M. Ashizawa, S. Uchida, T. Michinobu, *Macromol. Rapid Commun.* **2011**, *32*, 1804–1808; f) T. Michinobu, C. Seo, K. Noguchi, T. Mori, *Polym. Chem.* **2012**, *3*, 1427–1435; g) Y. Li, M. Ashizawa, S. Uchida, T. Michinobu, *Polym. Chem.*, **2012**, *3*, 1996–2005; h) T. Michinobu, *Syn. Org. Chem. Jpn.*, **2013**, *71*, 149–157.
- [8] a) T. Shoji, S. Ito, K. Toyota, M. Yasunami, N. Morita, *Chem. Eur. J.* **2008**, *14*, 8398–8408; b) T. Shoji, S. Ito, K. Toyota, T. Iwamoto, M. Yasunami, N. Morita, *Eur. J. Org. Chem.* **2009**, 4316–4324; c) T. Shoji, M. Maruyama, S. Ito, N. Morita, *Bull. Chem. Soc. Jpn.* **2012**, *85*, 761–773; d) T. Shoji, S. Ito, T. Okujima, N. Morita, *Org. Biomol. Chem.*, **2012**, *10*, 8308–8313; e) T. Shoji, S. Ito, T. Okujima, N. Morita, *Chem. Eur. J.* **2013**, *19*, 5721–5730.
- [9] a) T. Shoji, J. Higashi, S. Ito, T. Okujima, M. Yasunami, N. Morita, *Chem. Eur. J.* **2011**, *17*, 5116–5129; b) T. Shoji, J. Higashi, S. Ito, T. Okujima, M. Yasunami, N. Morita, *Org. Biomol. Chem.* **2012**, *10*, 2431–2438.
- [10] T. Shoji, S. Ito, T. Okujima, N. Morita, *Eur. J. Org. Chem.* **2011**, 5134–5140.
- [11] J.-P. Corbet, G. Mignani, *Chem. Rev.* **2006**, *106*, 2651–2710.
- [12] R. Boothe, C. Dial, R. Conaway, R. M. Pagni, G. W. Kabalka, *Tetrahedron Lett.* **1986**, *27*, 2207–2210.
- [13] a) S. M. Hubig, W. Jung, J. K. Kochi, *J. Org. Chem.* **1994**, *59*, 6233–6244; b) T. Mukaiyama, H. Kitagawa, J. Matsuo, *Tetrahedron Lett.* **2000**, *41*, 9383–9386.
- [14] a) K. J. Edgar, S. N. Falling, *J. Org. Chem.* **1990**, *55*, 5287–5291; b) G. A. Olah, G. Q. W. Sandford, P. G. K. Surya, *J. Org. Chem.* **1993**, *58*, 3194–3195; c) M. C. Carreno, J. L. G. Ruano, A. G. S. Miguel, A. Urbano, *Tetrahedron Lett.* **1996**, *37*, 4081–4084; d) A. S. Castanet, F. Colobert, P. E. Broutin, *Tetrahedron Lett.* **2002**, *43*, 5047–5048.
- [15] T. Yamamoto, K. Toyota, N. Morita, *Tetrahedron Lett.* **2010**, *51*, 1364–1366.
- [16] S. Kajigaeshi, T. Kakinami, H. Yamasaki, S. Fujisaki, T. Okamoto, *Bull. Chem. Soc. Jpn.* **1988**, *61*, 600–602.
- [17] a) Z.-H. Zhao, H. Jin, Y.-X. Zhang, Z. Shen, D.-C. Zou, X.-H. Fan, *Macromolecules* **2011**, *44*, 1405–1413; b) Y. Wu, H. Guo, T. D. James, J. Zhao, *J. Org. Chem.* **2011**, *76*, 5685–5695.
- [18] Y. Shirota, T. Kobata, N. Noma, *Chem. Lett.* **1989**, *18*, 1145–1148.
- [19] T. Shoji, E. Shimomura, M. Maruyama, S. Ito, T. Okujima, N. Morita, *Eur. J. Org. Chem.* **2013**, 957–964.
- [20] a) K. Sonogashira, Y. Tohda, N. Hagihara, *Tetrahedron Lett.* **1975**, *16*, 4467–4470; b) S. Takahashi, Y. Kuroyama, K. Sonogashira, N. Hagihara, *Synthesis* **1980**, 627–630; c) K. Sonogashira, Coupling reactions between sp² and sp carbon centers, in *Comprehensive Organic Synthesis*, vol. 3 (Eds.: B. M. Trost, I. Fleming), Pergamon, Oxford, **1991**, chapter 2.4, p. 521–549; d) K. Sonogashira, Cross-coupling reactions to sp carbon atoms, in *Metal-Catalyzed Cross-Coupling Reactions* (Eds.: F. Diederich, P. J. Stang), Wiley-VCH, Weinheim, Germany, **1998**, chapter 5, p. 203–229.
- [21] M. Jordan, M. Kivala, C. Boudon, J.-P. Gisselbrecht, W. B. Schweizer, P. Seiler, F. Diederich, *Chem. Asian J.* **2011**, *6*, 396–401.
- [22] M. Kivala, C. Boudon, J.-P. Gisselbrecht, P. Seiler, M. Gross, F. Diederich, *Chem. Commun.* **2007**, 4731–4733.
- [23] a) P. Suppan, N. Ghoneim, *Solvatochromism*, Royal Society of Chemistry, Cambridge, **1997**; b) P. Suppan, *J. Photochem. Photobiol., A*, **1990**, *50*, 293–330; c) C. Reichardt, *Solvent and Solvent Effects in Organic Chemistry*, Wiley-VCH, New York, **2004**.
- [24] The B3LYP/6-31G(d) time-dependence density functional calculations were performed with Spartan¹⁰, Wavefunction, Irvine, CA.

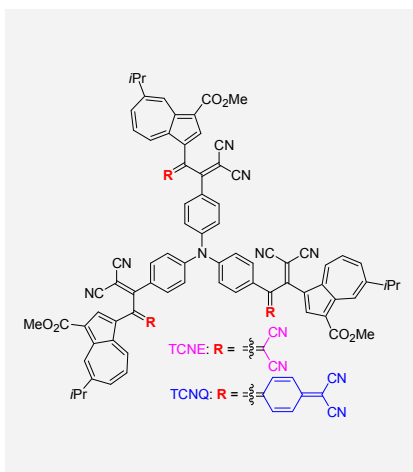
- [25] (a) S. Ito, N. Morita, *Eur. J. Org. Chem.* **2009**, 4567–4579; (b) S. Ito, T. Shoji, N. Morita, *Synlett* **2011**, *16*, 2279–2298.

Received: ((will be filled in by the editorial staff))
Published online: ((will be filled in by the editorial staff))

Entry for the Table of Contents ((Please choose one layout.))

Azulene Chemistry

1-Ethynylazulenes connected by several arylamine cores reacted with TCNE and TCNQ in a formal [2 + 2] cycloaddition to afford the corresponding tetracyanobutadiene and dicyanoquinodimethane chromophores, respectively. The redox behavior of the novel chromophores was examined by cyclic voltammetry, which revealed their multistep electrochemical reduction properties. Moreover, a significant color changes were observed by visible spectroscopy under the electrochemical reduction conditions.



Taku Shoji,* Erika Shimomura, Mitsuhsa Maruyama, Akifumi Maruyama, Shunji Ito, Tetsuo Okujima, Koza Toyota, and Noboru Morita Page No. – Page No.

Synthesis and Properties of Azulene-substituted Donor–Acceptor Chromophores Connected by Arylamine Cores

Keywords: Azulene / Arylamine / π -Conjugate system / Cycloaddition / Redox chemistry

